

(12)
FG

See 1473

Project Report

TT-8

R. J. Becherer

Pulsed Laser Ranging Techniques
at 1.06 and 10.6 μm

19 March 1976

Prepared for the Defense Advanced Research Projects Agency
under Electronic Systems Division Contract F19628-76-C-0002 by

Lincoln Laboratory

MASSACHUSETTS INSTITUTE OF TECHNOLOGY

LEXINGTON, MASSACHUSETTS



Approved for public release; distribution unlimited.

DDC
RECORDED
MAY 20 1976
REGULATED
B

AD A 024557

**BEST
AVAILABLE COPY**

The work reported in this document was performed at Lincoln Laboratory, a center for research operated by Massachusetts Institute of Technology. This work was sponsored by the Defense Advanced Research Projects Agency under Air Force Contract F19628-76-C-0002 (ARPA Order 2752).

This report may be reproduced to satisfy needs of U.S. Government agencies.

The views and conclusions contained in this document are those of the contractor and should not be interpreted as necessarily representing the official policies, either expressed or implied, of the Defense Advanced Research Projects Agency of the United States Government.

ACCESSION for	
NTIS	White Section <input checked="" type="checkbox"/>
DOC	Buff Section <input type="checkbox"/>
UNANNOUNCED	<input type="checkbox"/>
JUSTIFICATION	
.....	
BY	
DISTRIBUTION/AVAILABILITY CODES	
Dist.	As ALL and/or SPECIAL
A	

This technical report has been reviewed and is approved for publication.

FOR THE COMMANDER

Eugene C. Raabe

Eugene C. Raabe, Lt. Col., USAF
Chief, ESD Lincoln Laboratory Project Office

MASSACHUSETTS INSTITUTE OF TECHNOLOGY
LINCOLN LABORATORY

PULSED LASER RANGING TECHNIQUES AT 1.06 AND 10.6 μm

R. J. BECHERER
Group 53

PROJECT REPORT TT-8

19 MARCH 1976

Approved for public release; distribution unlimited.

LEXINGTON

MASSACHUSETTS

ABSTRACT

Heterodyne and direct detection pulsed laser range finders at both 1.06 and 10.6 μm are compared. The comparison includes determination of the laser power required to achieve useful signal-to-noise ratios at ranges between 1 and 10 km.

The application of interest involves a transmitter/receiver with a single aperture located approximately at ground level ranging on unresolved targets which appear at a few degrees above horizontal against a sky or terrain background.

Performance factors analyzed include backgrounds, beam coherence reduction due to turbulence, scintillation, beam steering and spreading, and atmospheric transmittance. The atmospheric transmittance effects are based on recent analysis of real weather data.

Available and projected CO₂ and Nd: YAG power levels are assessed to determine expected operating ranges for typical systems.

CONTENTS

ABSTRACT	iii
LIST OF ILLUSTRATIONS	vi
LIST OF TABLES	vii
1. INTRODUCTION AND CONCLUSIONS	1
2. PERFORMANCE FACTORS	5
2.1 Signal-to-Noise and Range Loss	5
2.2 Backgrounds	9
2.3 Atmospheric Transmittance and Weather	12
2.4 Atmospheric Turbulence	14
2.4.1 Beam Coherence Reduction	15
2.4.2 Scintillation	18
2.4.3 Other Effects	27
3. LASER POWER REQUIREMENTS	28
APPENDIX A	37
REFERENCES	39

LIST OF ILLUSTRATIONS

Fig. 1. Background power collected by receiver.	11
Fig. 2. Coherence diameter for heterodyne receiver.	17
Fig. 3. Log-intensity correlation distance.	20
Fig. 4a. Variance of log-intensity vs. range.	21
Fig. 4b. Normalized std. deviation of signal due to atmospheric scintillation.	24
Fig. 4c. Normalized std. deviation of signal due to atmospheric scintillation.	25
Fig. 5. RMS angular beam spread due to turbulence.	29
Fig. 6. Range loss factor vs. range.	31
Fig. 7. Required laser power P_T to achieve $SNR_p = 50$.	35

LIST OF TABLES

Table 1.	Background Spectral Radiance N_λ	10
Table 2.	Atmospheric Attenuation Values from McClatchey et al	13
Table 3.	Annual Average Attenuation and Seasonal Range in dB/km	13
Table 4.	Normalized Variance of Signal After Aperture Averaging (Direct Detection, $\lambda = 1.06\mu\text{m}$)	23
Table 5.	Normalized variance of Signal (Direct Detection, $\lambda = 10.6\mu\text{m}$, $\theta = 0.$)	23
Table 6.	System Parameters for Direct and Heterodyne Systems at 1.06 and 10.6 μm	32
Table 7.	Direct Detection NEP/Hz ^{1/2} at 1.06 and 10.6 μm	33

1. INTRODUCTION AND CONCLUSIONS

Nd:YAG laser range finders employing direct detection techniques at $1.06\mu\text{m}$ are now widely used. The purpose of this technical note is to compare the signal-to-noise characteristics and ranging capabilities of these systems with the characteristics and capabilities of alternative systems which would use a CO_2 laser. The CO_2 system would operate on the P20 line at $10.591\mu\text{m}$ and would employ either direct or heterodyne detection.

There are several apparent advantages in using the CO_2 laser for range finding. Among these advantages is the generally high atmospheric transmission available at $10.6\mu\text{m}$. The $10.6\mu\text{m}$ laser beam is known to be less attenuated by atmospheric aerosols than the $1.06\mu\text{m}$ beam. As a result it more easily penetrates light fog and is relatively insensitive to atmospheric haze levels.

Another advantage of the CO_2 laser is that at $10.6\mu\text{m}$ it is possible to achieve the very large conversion gains available with heterodyne detection techniques. The alignment of a heterodyne system is ten times less critical at $10.6\mu\text{m}$ than at $1.06\mu\text{m}$. Also, at the longer wavelength the atmospheric turbulence effects on the spatial coherence of the laser beam wavefront entering the detector are twenty-five times less important. These differences insure that a CO_2 heterodyne ranging system can be used under field conditions which would prohibit the use of a Nd: YAG heterodyne system. The heterodyne gain advantages also suggest that a CO_2 heterodyne system would achieve substantially greater ranges with improved range accuracy

over comparable presently available Nd: YAG direct detection range finders.

Recent infrared detector improvements support the use of heterodyne techniques with the CO₂ laser. HgCdTe photovoltaic detectors with 1 GHz bandwidth have recently been developed. The technology of detector array fabrication has developed rapidly. Charge coupled and charge injection array devices have been demonstrated and are receiving high levels of support to increase array size. This array technology will permit the construction of infrared heterodyne receivers with high conversion efficiency and covering a large instantaneous field of view in the near future.

Another direct factor of major importance in considering CO₂ laser ranging systems is the recent rapid improvement in the technology of high pulse power, high efficiency, compact sealed off CO₂ lasers. These devices are usually low repetition rate systems and are therefore ideally suited to the ranging application. For example, a device with 1.0 MW peak power in a 50 ns pulse with operating lifetime exceeding 10⁶ pulses has recently been reported in the literature. This device is less than 35 cm in length.

The approach taken in this technical note in comparing the performance of direct and heterodyne detection techniques at both 1.06μm and 10.6μm is to first analyze the factors which play a major role in determining the system performance. These factors include the losses associated with the geometry of the ranging problem including target cross section, beam divergence, receiver aperture area, and range. They also include an assessment of background radiation levels, atmospheric transmission effects, and the impact of atmospheric turbulence phenomena such as beam coherence

reduction, scintillation, beam steering, and beam spreading.

The final assessment of the relative merit of the two detection techniques and the two wavelengths of operation requires the calculation of the radiated power level of the laser transmitter required to achieve a 17 dB single pulse signal-to-noise power ratio for operation at ranges up to 10 km. These requirements are then compared with available power levels of Nd:YAG and CO₂ pulsed lasers.

The application of interest here involves a transmitter/receiver with a common aperture located approximately at ground level ranging on unresolved targets which appear at a few degrees above horizontal against a sky or terrain background.

The principal conclusions of this analysis are as follows:

1. Direct detection techniques are preferable to heterodyne techniques at $\lambda = 1.06\mu\text{m}$. This is principally due to the beam coherence reduction and scintillation fading effects induced by atmospheric turbulence at this wavelength in the near-ground level application.
2. Direct detection systems at $10.6\mu\text{m}$ require less laser power than direct detection systems at $1.06\mu\text{m}$, primarily due to statistically higher atmospheric transmission at the longer wavelength. The advantage is approximately 20 dB at 10 km range in a typical situation.
3. Heterodyne detection techniques at $10.6\mu\text{m}$ offer very large advantages in required laser power over direct detection techniques at either $1.06\mu\text{m}$ or $10.6\mu\text{m}$. The advantage over the 1.06 direct detection system is partly due to the higher atmospheric transmission at

10.6 μ m but is primarily due to the low noise and high gain of the heterodyne method. The advantage in dB is shown in the following table for a typical situation.

	<u>1 km</u>	<u>5 km</u>	<u>10 km</u>
1.06 direct	reference	reference	reference
10.6 direct	1.4	10.2	21.2
10.6 heterodyne	37.1	45.9	56.9

4. Scintillation fading can be significant at ranges greater than 5 km with near-ground level systems. This effect is present when using either heterodyne or direct detection. In a typical situation when the turbulence is characterized by a refractive index structure parameter $C_N^2 = 10^{-15} m^{-2/3}$ the fading is estimated to be 20 to 30% at 5 km range.
5. Beam spreading and steering effects for a 0.1 milliradian beam at $\lambda = 10.6\mu$ m are expected to be negligible under essentially all turbulence conditions at ranges up to 10 km. At 1.06 μ m the same beam divergence angle leads to negligible beam spreading and steering for all C_N^2 less than $3 \times 10^{-15} m^{-2/3}$ at ranges up to 10 km. For C_N^2 larger than this value the spreading and/or steering effects can be significant at the shorter wavelength.

These conclusions regarding the superior performance of heterodyne detection at 10.6 μ m must be weighed against the added requirement for a local oscillator laser and the additional signal processing required. Also, the conclusions apply to range finders employing pulses in the 10ns to 1 μ s range. For pulse lengths much less than 1ns the direct detection techniques begin to

compare more favorably with the CO₂ heterodyne techniques.

2. PERFORMANCE FACTORS

2.1 Signal-to-Noise and Range Loss

The most important measure of performance is signal-to-noise ratio (SNR)*. The electrical power SNR for direction detection is

$$\text{SNR}_p = \frac{i_s^2}{i_N^2} = \frac{i_s^2}{i_{SN}^2 + i_{BN}^2 + i_{DN}^2 + i_{TN}^2 + i_{AN}^2} \quad (1)$$

where i_N^2 is the mean square noise current composed of shot noise of the signal, shot noise of the background, shot noise of the dark current, thermal noise, and amplifier noise. For heterodyne detection local oscillator shot noise dominates all other noise sources so that for heterodyne detection

$$\text{SNR}_p = \frac{i_s^2}{i_N^2} = \frac{i_s^2}{i_{LN}^2} \quad (2)$$

where i_{LN}^2 is the mean square noise current due to the shot noise of the local oscillator.

The complete form of these signal-to-noise ratios is as follows. For direct detection with a photovoltaic detector

$$\text{SNR}_p = \frac{G^2 R^2 P_R^2}{2 q G^2 F' (R P_R + R P_B + I_D) B + \frac{4k T B}{R} + \frac{4(F-1)k T_{290} B}{R}} \quad (3)$$

*Direct detection SNR is at detector output, heterodyne SNR is at the intermediate frequency.

where

G = gain of detector

R = current responsivity of detector

P_R = received optical signal power

q = electronic charge

F' = detector gain mechanism noise factor

P_B = received optical background power

I_D = dark current

B = noise bandwidth

k = Boltzmann constant

T = temperature of load resistor

R = Load resistance

F = noise factor of amplifier

T_{290} = 290K reference temperature

The equivalent expression for heterodyne detection is

$$SNR_p = \frac{\eta P_R}{h \nu B} \quad (4)$$

where

η = quantum efficiency

h = Planck constant

ν = frequency of local oscillator

Under most conditions of interest for direct detection the signal shot noise is small in comparison with other noise sources. The SNR_p for direct

detection can then be expressed in a convenient way as

$$\text{SNR}_p = \left(\frac{P_R}{\text{NEP}} \right)^2 = \left(\frac{P_R}{\text{NEP/Hz}^{1/2} \cdot B^{1/2}} \right)^2 \quad (5)$$

where NEP, the noise equivalent power, or $\text{NEP/Hz}^{1/2}$ is used as a measure of detector noise. For comparison the signal-to-noise ratio in heterodyne detection is

$$\text{SNR}_p = \frac{P_R}{h \nu B/\eta} \quad (6)$$

Notice that while the SNR_p for both methods of detection is inversely proportional to bandwidth, the received signal power P_R required to produce a given SNR_p is proportional in one case to $B^{1/2}$ and in the second case to B . In this evaluation of the two detection methods we take the approach of determining the power P_R required to produce a given SNR_p .

The range loss is the ratio of received to transmitted power. This ratio is

$$L_R = \frac{P_R}{P_T} = \frac{\sigma}{\theta^2 R^2} \cdot e^{-2 \alpha R} \cdot \frac{A}{\pi R^2} \cdot \epsilon \quad (7)$$

where

P_R = received optical signal power

P_T = transmitted optical signal power

σ = target cross section

θ = angular size of transmitted beam

R = range

α = atmospheric attenuation coefficient

A = area of receiver aperture

ϵ = optical efficiency (lenses, filters, alignment, etc)

In general, the range loss for heterodyne and direct detection systems shows the same dependence on the parameters listed. However, the largest receiver aperture which can be used is limited by the return beam coherence requirement for heterodyne detection. Also the optical efficiency is different due to tighter alignment requirements for the heterodyne detection system.

Since the range loss and the transmitted power determine the received power, the SNR_p and range loss equations can be combined for direct detection,

$$\text{SNR}_p = \left[\frac{P_T}{\text{NEP}} \cdot L_R \right]^2 = \left[\frac{P_T}{\text{NEP}} \cdot \frac{\sigma}{\theta^2 R^2} \cdot e^{-2\alpha R} \cdot \frac{A}{\pi R^2} \cdot \epsilon \right]^2 \quad (8)$$

and for heterodyne detection,

$$\text{SNR}_p = \frac{P_T}{h \nu B/\eta} \cdot L_R = \frac{P_T}{h \nu B/\eta} \cdot \frac{\sigma}{\theta^2 R^2} \cdot e^{-2\alpha R} \cdot \frac{A}{\pi R^2} \cdot \epsilon \quad (9)$$

The dependence on the system parameters is different if we fix P_T and calculate SNR_p versus the approach of fixing SNR_p and calculating the required transmitter power P_T .

The present evaluation of ranging techniques will provide more useful results by taking the approach of specifying the desired SNR_p to achieve adequate range measurement and then calculating the required power P_T .

There are two reasons for this. First, the magnitude of the signal-to-noise ratios is of no particular interest once the minimum ratio required to accomplish the system objective has been reached. Second, the state of laser technology is improving rapidly and any assumption of a particular laser power value would be quickly out of date. It is more useful to have system performance stated in the form of laser power required vs. range so that as available laser powers increase the increased operating range can be readily determined.

The following parts of this section of the report present an assessment of those hardware and environment factors which have an impact on the laser power required to achieve adequate signal-to-noise ratio.

2.2 Backgrounds

One of the advantages of heterodyne detection is that it provides very high levels of spatial and spectral discrimination against background radiation. As a result background radiation levels are unimportant in all but the most extreme situations such as a receiver looking directly at the sun.

With direct detection background radiation must be considered. At $1.06\mu\text{m}$ the principle background is scattered solar radiation. At $10.6\mu\text{m}$ it is thermal emission from the environment at ambient temperature - usually approximately 300K.

In a typical application the range finder is at ground level and the target appears at an elevation angle above horizontal against a sky

background. Typical values of background spectral radiance¹ are shown in Table 1.

TABLE 1

Wavelength	BACKGROUND SPECTRAL RADIANCE N_λ			
	Scattering (Clear Sky)	Sunlit Cloud	6000K Sun	300K Sky
1.06 μm	2.5×10^{-8}	7×10^{-7}	8×10^{-2}	----
	$\text{w.m}^{-2} \cdot \text{sr}^{-1} \cdot \mu\text{m}^{-1}$			
10.6 μm	-----	-----	2×10^{-5}	10^{-7}

The received optical background power exclusive of optical system transmission effects is

$$P_B' = N_\lambda A \theta^2 \Delta\lambda \quad (10)$$

where

N_λ = spectral radiance

A = receiver aperture area

θ = acceptance angle of receiver

$\Delta\lambda$ = wavelength interval

For this evaluation we consider a 10 cm diameter receiving aperture and $\Delta\lambda = \lambda/100$. These are reasonable values for a portable range finder with a narrow band interference filter to minimize background radiation noise. The received background power P_B' under these conditions is shown as a function of θ in Figure 1. The acceptance angle θ may be determined by

(1) diffraction

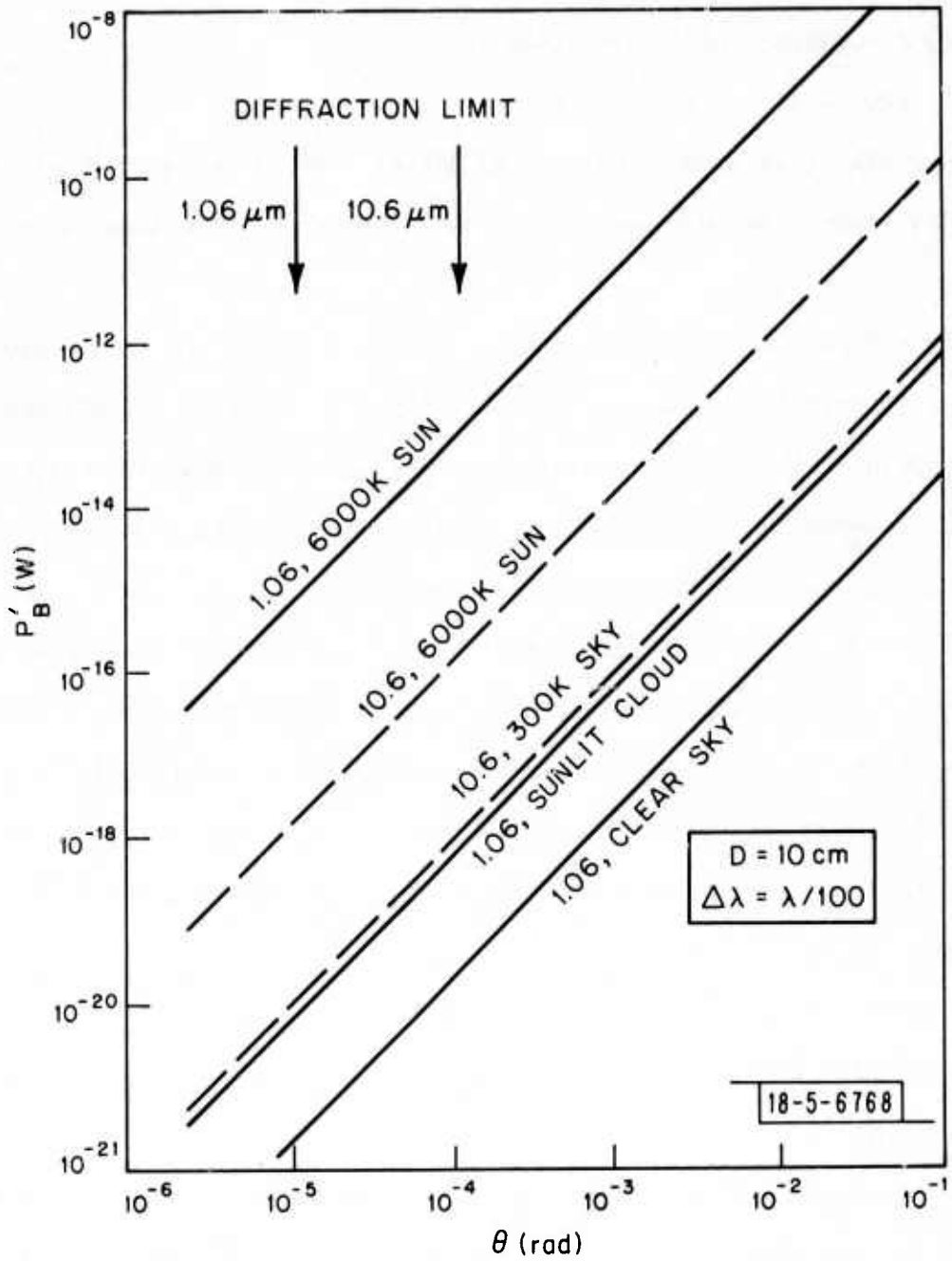


Fig. 1. Background power collected by receiver.

- (2) atmospheric beam spreading, or
- (3) cueing accuracy to the range finder.

For this analysis we assume that the essential limitations are either (1) or (2). This report does not address the question of the effect of cueing accuracy.

The diffraction limited acceptance angles for 1.06 and 10.6 μ m wavelengths with this 10 cm aperture are also shown in Figure 1. Atmospheric beam spreading will increase the acceptance angle. The magnitude of this increase is determined in the section on atmospheric turbulence.

2.3 Atmospheric Transmittance and Weather

At 1.06 μ m the primary cause of attenuation is aerosol scattering and absorption with a relatively small contribution also from molecular scattering. At this wavelength molecular absorption effects are negligible.

At 10.6 μ m molecular resonance absorption and molecular scattering are the dominant loss mechanisms with aerosol absorption and scattering of less importance.

Attenuation in rain² at 10.6 m is approximately the same as 1.06 μ m, although at 10.6 μ m this is due to absorption while at 1.06 μ m scattering is more important.

Typical attenuations in dB/km as determined by McClatchey³ are shown in Table 2. The clear and hazy day aerosol models correspond to visibilities of 23 and 5 km, respectively, at ground level.

TABLE 2

ATMOSPHERIC ATTENUATION VALUES FROM McCLATCHEY ET AL³

<u>Condition</u>	Total Attenuation (dB/km)	
	<u>$\lambda = 1.06\mu\text{m}$</u>	<u>$\lambda = 10.6\mu\text{m}$</u>
Midlatitude summer, clear	0.384	1.72
Midlatitude winter, clear	0.385	0.459
Midlatitude summer, hazy	1.86	1.88
Midlatitude winter, hazy	1.86	0.627

Table 3 shows annual average attenuation and approximate seasonal range in dB/km at four sites in Germany for 50 and 80% confidence levels from recent work by Kleiman and Modica.⁴ These attenuations are obtained by calculation from real weather data contained in the Rand Weather Data Bank (RAWDAB). At 80% confidence level the attenuation is less than the value shown 80% of the time.

TABLE 3

ANNUAL AVERAGE ATTENUATION AND SEASONAL RANGE IN dB/km

Site	<u>$\lambda = 1.06\mu\text{m}$</u>		<u>$\lambda = 10.6\mu\text{m}$</u>	
	50%	80%	50%	80%
Berlin	1.63 ± 0.3	2.11 ± 0.65	0.913 ± 0.25	1.44 ± 0.10
Dresden	2.15 ± 0.4	3.00 ± 0.5	1.088 ± 0.25	1.68 ± 0.20
Hamburg	1.69 ± 0.15	2.69 ± 0.8	1.025 ± 0.20	1.48 ± 0.20
Essen	1.70 ± 0.15	2.81 ± 0.8	1.088 ± 0.25	1.60 ± 0.30
Average	1.80	2.65	1.03	1.55

Direct comparison of the two sets of data is not possible. McClatchey's models are derived from the U.S. Standard Atmosphere of 1962 and the Supplemental Atmospheres while the Kleiman and Modica results are derived directly from real weather data taken in Central Europe. In the following we use the Kleiman and Modica average results.

Some general conclusions regarding the effects of weather are apparent from the McClatchey and the Kleiman and Modica results. McClatchey's results show that aerosols play a dominant role at $1.06\mu\text{m}$. The total attenuation determined by McClatchey for the midlatitude winter hazy day model at $1.06\mu\text{m}$ is 1.86 dB/km. This is approximately equal to the 1.80 dB/km attenuation determined by Kleiman and Modica for 50% of the weather situations in Germany. This indicates that the seasonal average weather effects in Germany at $\lambda = 1.06\mu\text{m}$ are similar to those of a hazy day represented by the U.S. Standard Atmosphere and 5 km visibility.

At $\lambda = 10.6\mu\text{m}$ it is apparent that McClatchey's summer and winter results are greater and less, respectively, than the Kleiman and Modica seasonal average for 50% of the situations. However, if McClatchey's summer and winter results are averaged and treated as a seasonal average the results are close to the 50% results of Kleiman and Modica at this wavelength. The agreement is essentially independent of the aerosol content within the 5-23 km visibility range. This indicates that the seasonal average weather effects in Germany at $\lambda = 10.6\mu\text{m}$ are similar to those represented by the U.S. Standard Atmosphere and visibilities between 5 and 23 km.

2.4 Atmospheric Turbulence

Atmospheric turbulence causes beam coherence reduction, scintillation, and beam steering and spreading. The first effect is most important in heterodyne detection which requires constructive interference between the signal beam and the local oscillator beam. The same physical phenomena which cause beam coherence reduction in heterodyne detection cause image dancing and blurring in direct detection.

Scintillation affects both direct and heterodyne receivers. It causes temporal fluctuations of the signal power level which can be described as a rapid random modulation or fading of the signal. This effect is minimized in the direct detection system by using as large an aperture as possible to achieve aperture averaging of scintillation.⁵ However, in the heterodyne detection system⁶ the aperture can be increased only until the receiver diameter is approximately equal to the coherence diameter of the wavefront. Further increase only leads to increased modulation noise due to loss of heterodyne signal efficiency.

Beam steering in the radar or range finder application is usually important only between the transmitter and the target, not between the target and receiver. A specular target is the exception.

2.4.1 Beam Coherence Reduction

The analysis of clear air propagation effects⁷ for plane waves in a homogeneous locally isotropic medium shows that the wave structure function $D(r)$ which describes the loss of coherence is

$$D(r) = \begin{cases} 1.46 \\ 2.92 \end{cases} C_N^2 k^2 R r^{5/3} \quad (11)$$

where r is the separation of the two observation points, C_N^2 is the refractive index structure parameter which is a measure of the intensity of the refractive index fluctuations, $k = 2\pi/\lambda$, and R is the range. In the bracket the upper constant applies when the source is in the far field of the observation points, i.e., when $R \gg r^2/\lambda$, and the lower constant applies when the source is in the near field, i.e., when $R \leq r^2/\lambda$.

For an aperture of 10 cm diameter, the far field distance is 10 km for $\lambda = 1.06\mu\text{m}$ and 1 km for $\lambda = 10.6\mu\text{m}$. Typical ranges of interest are between 1 and 10 km. The $10.6\mu\text{m}$ systems then usually operate in the far field.

The beam coherence reduction due to turbulence can be characterized by a coherence diameter r_0 . When the diameter of the receiving aperture is $r = r_0$ the signal conversion efficiency of the heterodyne receiver has dropped 3.5 dB from the ideal efficiency of a completely coherent beam.⁸

This coherence diameter is

$$r_0 = \begin{cases} 2.53 \\ 1.67 \end{cases} C_N^{-6/5} k^{-6/5} R^{-3/5} \quad (12)$$

where again the upper constant applies when the source is in the far field of the observation points.

Figure 2 shows the coherence diameter r_0 as a function of range for $\lambda = 10.6\mu\text{m}$ and for various values of C_N^2 corresponding to strong, intermediate, and weak turbulence near ground level. Strong turbulence usually occurs in clear weather on sunny days since temperature differences due to heating are greatest at this time, and refractive index fluctuations are caused almost exclusively by fluctuations in temperature.

Figure 2 shows that under all but the most extreme turbulence condition the 10 cm diameter receiving aperture is smaller than the coherence diameter due to turbulence at ranges up to 10 km. The C_N^2 values shown in this figure correspond to measured values of C_N^2 within a few meters of ground level.⁹ Consider a situation in which the target appears at an elevation

Scintillation affects both direct and heterodyne receivers. It causes temporal fluctuations of the signal power level which can be described as a rapid random modulation or fading of the signal. This effect is minimized in the direct detection system by using as large an aperture as possible to achieve aperture averaging of scintillation.⁵ However, in the heterodyne detection system⁶ the aperture can be increased only until the receiver diameter is approximately equal to the coherence diameter of the wavefront. Further increase only leads to increased modulation noise due to loss of heterodyne signal efficiency.

Beam steering in the radar or range finder application is usually important only between the transmitter and the target, not between the target and receiver. A specular target is the exception.

2.4.1 Beam Coherence Reduction

The analysis of clear air propagation effects⁷ for plane waves in a homogeneous locally isotropic medium shows that the wave structure function $D(r)$ which describes the loss of coherence is

$$D(r) = \begin{cases} 1.46 \\ 2.92 \end{cases} C_N^2 k^2 R r^{5/3} \quad (11)$$

where r is the separation of the two observation points, C_N^2 is the refractive index structure parameter which is a measure of the intensity of the refractive index fluctuations, $k = 2\pi/\lambda$, and R is the range. In the bracket the upper constant applies when the source is in the far field of the observation points, i.e., when $R \gg r^2/\lambda$, and the lower constant applies when the source is in the near field, i.e., when $R \leq r^2/\lambda$.

For an aperture of 10 cm diameter, the far field distance is 10 km for $\lambda = 1.06\mu\text{m}$ and 1 km for $\lambda = 10.6\mu\text{m}$. Typical ranges of interest are between 1 and 10 km. The $10.6\mu\text{m}$ systems then usually operate in the far field.

The beam coherence reduction due to turbulence can be characterized by a coherence diameter r_0 . When the diameter of the receiving aperture is $r = r_0$ the signal conversion efficiency of the heterodyne receiver has dropped 3.5 dB from the ideal efficiency of a completely coherent beam.⁸ This coherence diameter is

$$r_0 = \begin{cases} 2.53 \\ 1.57 \end{cases} C_N^{-6/5} k^{-6/5} R^{-3/5} \quad (12)$$

where again the upper constant applies when the source is in the far field of the observation points.

Figure 2 shows the coherence diameter r_0 as a function of range for $\lambda = 10.6\mu\text{m}$ and for various values of C_N^2 corresponding to strong, intermediate, and weak turbulence near ground level. Strong turbulence usually occurs in clear weather on sunny days since temperature differences due to heating are greatest at this time, and refractive index fluctuations are caused almost exclusively by fluctuations in temperature.

Figure 2 shows that under all but the most extreme turbulence condition the 10 cm diameter receiving aperture is smaller than the coherence diameter due to turbulence at ranges up to 10 km. The C_N^2 values shown in this figure correspond to measured values of C_N^2 within a few meters of ground level.⁹ Consider a situation in which the target appears at an elevation

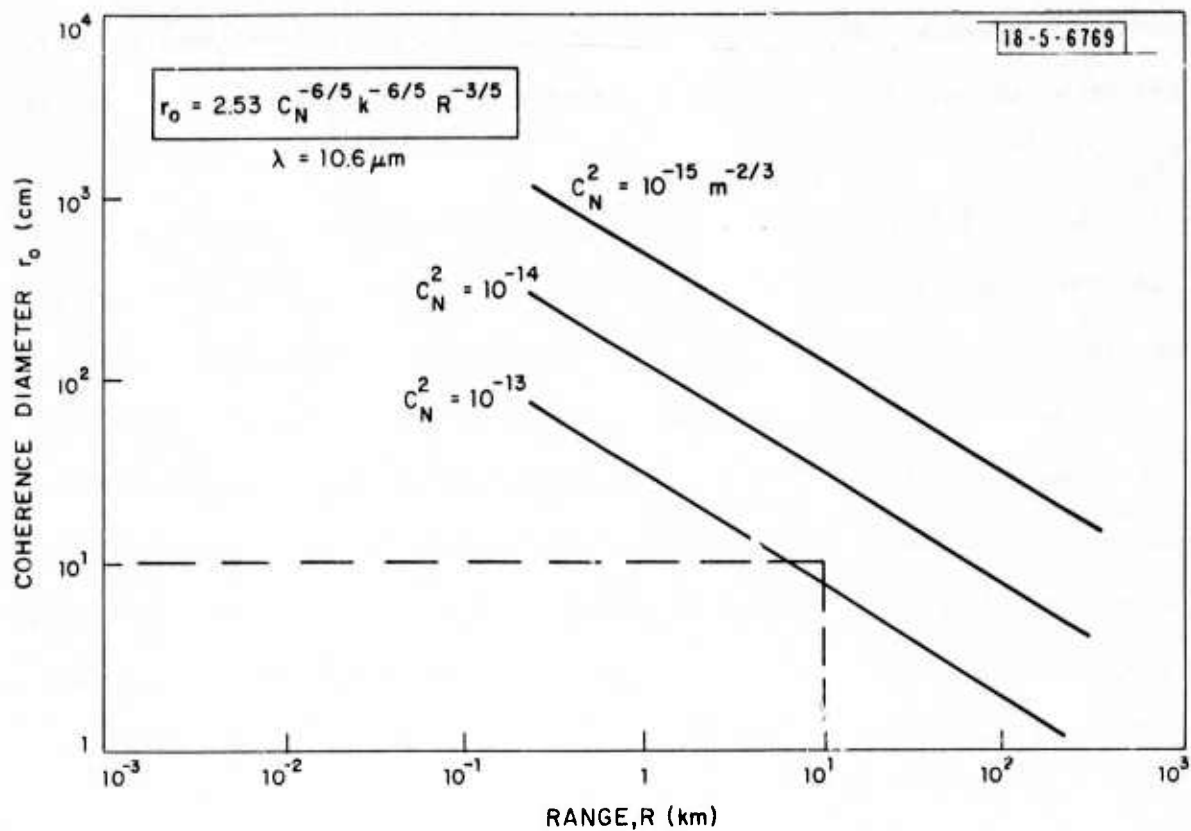


Fig. 2. Coherence diameter for heterodyne receiver.

angle above the horizontal. The effective value of C_N^2 is then approximately the average value over the path between target and receiver. Since C_N^2 is known to decrease rapidly above the first thirty meters from ground level, effective values of C_N^2 under worst conditions may actually be smaller than $C_N^2 = 10^{-13}$.

We conclude that with a 10 cm diameter receiving aperture the heterodyne efficiency losses at $10.6\mu\text{m}$ due to atmospheric turbulence can be expected to be no greater than 3.5 dB under almost all field conditions.

However, at $1.06\mu\text{m}$ the coherence diameter is reduced by a factor of 25 from the values at $10.6\mu\text{m}$. This reduction is shown in equation 12. Under the same atmospheric turbulence condition a 0.4 cm diameter receiving aperture at $1.06\mu\text{m}$ corresponds to the 10 cm aperture at $10.6\mu\text{m}$. The energy collection performance of this small aperture severely restricts the performance of a heterodyne receiver for use with a Nd:YAG transmitter.

2.4.2 Scintillation

Scintillation is a random modulation of the received signal power level due to atmospheric turbulence. Except at very high transverse wind speeds the temporal power spectrum of scintillation is usually limited to less than 1 KHz. The effect of scintillation on a pulsed laser range finder is therefore to produce a random pulse-to-pulse amplitude modulation since the pulse duration is much shorter than the scintillation time. Laser power levels must be selected to produce adequate SNR over the range of received power fluctuations.

The magnitude of scintillation is characterized by $\sigma_{\ln I}^2$, the variance of log-intensity. For a plane wave in a homogeneous isotropic medium,

$$\sigma_{\ln I}^2 = 1.23 C_N^2 k^{7/6} R^{11/6} \quad (13)$$

where C_N^2 is the refractive index structure parameter, $k = 2\pi/\lambda$ and R is the range. Equation 13 assumes that the receiver is a point receiver. This is essentially true when the receiver diameter is smaller than the transverse correlation distance of the log-intensity fluctuations. This distance is approximately equal to $\sqrt{\lambda R}$, the radius of the first Fresnel zone.*

Figure 3 shows the correlation distance $\sqrt{\lambda R}$ as a function of range for the two wavelengths 1.06 and 10.6 μm . The figure shows that at $\lambda = 10.6\mu\text{m}$ the 10 cm receiver diameter is smaller than the log-intensity correlation distance at ranges greater than 1 km. Then equation 13 is essentially correct at this wavelength and describes the expected magnitude of scintillation at the detector.

Figure 4a shows $\sigma_{\ln I}^2$ for $\lambda = 10.6\mu\text{m}$. Experimental data¹⁰ shows that the variance of log-intensity saturates at approximately 2.5.

However, at $\lambda = 1.06\mu\text{m}$ Figure 3 shows that the 10 cm receiver diameter is larger than $\sqrt{\lambda R}$ at all ranges less than 10 km. This means that aperture averaging of scintillation occurs at this wavelength. To estimate the effects

*The log intensity correlation distance is strictly equal to $\sqrt{\lambda R}$ for weak turbulence such that $\sigma_{\ln I}^2 \ll 1$.

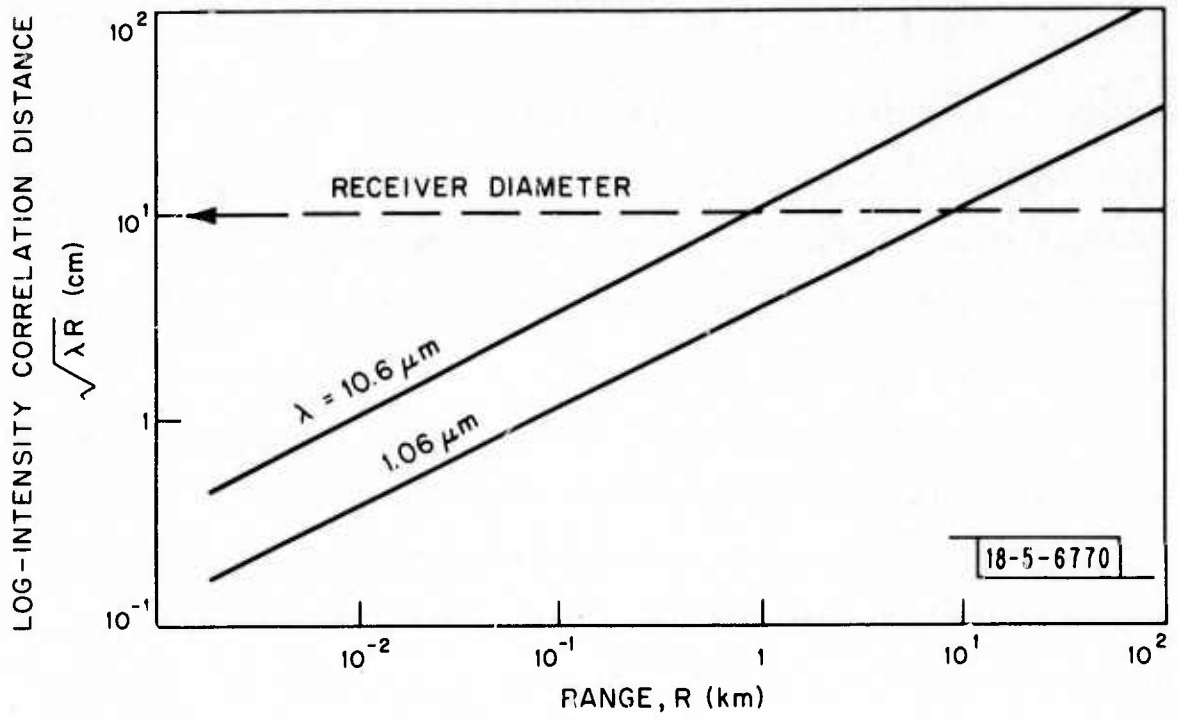


Fig. 3. Log-intensity correlation distance.

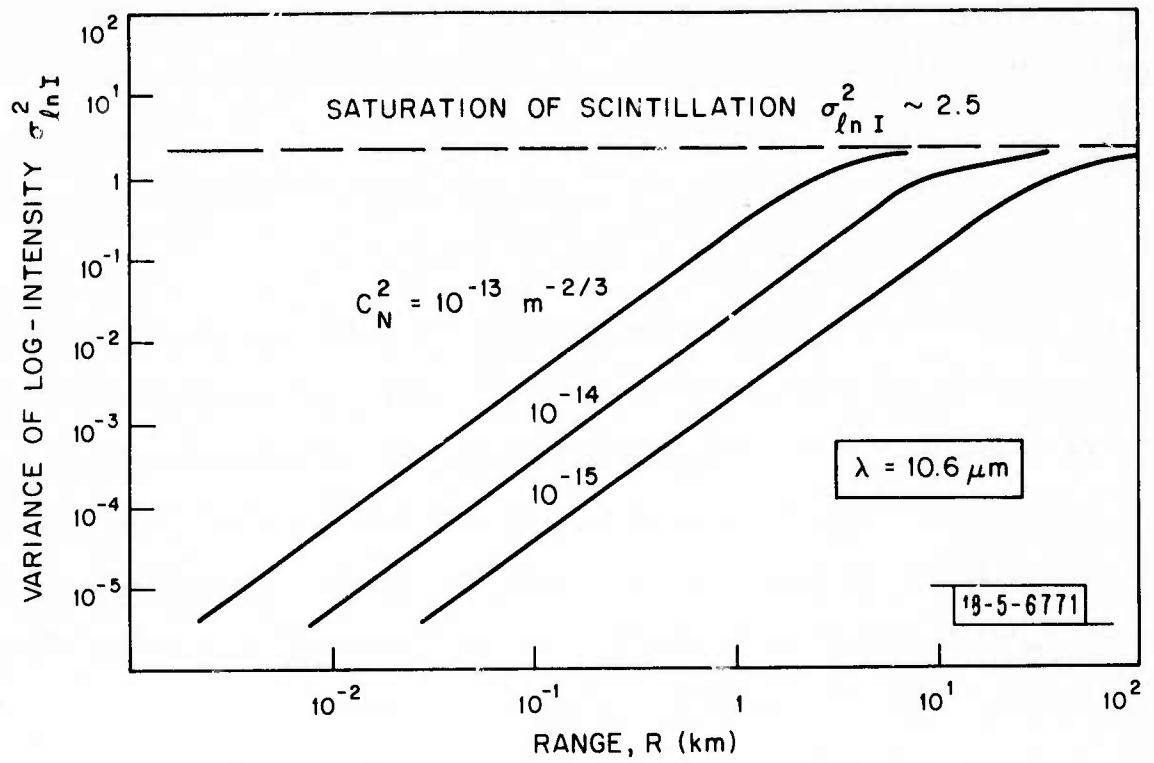


Fig. 4a. Variance of log-intensity vs. range.

of aperture averaging we must distinguish between heterodyne and direct detection.

For direct detection the normalized variance of the signal, either current or voltage, measured by the detector is

$$\frac{\sigma_s^2}{\bar{s}^2} = \Theta \left[\exp(\sigma_{\ln I}^2) - 1 \right] \quad (14)$$

where \bar{s} is the average signal level and Θ is the aperture averaging factor. Values of Θ can be determined from graphical results presented in reference 5. Table 4 shows σ_s^2 / \bar{s}^2 as a function of range for various values of C_N^2 representing strong, intermediate, and weak turbulence at ground level.

At 10.6 μ m the corresponding values of normalized signal variance can be estimated from equation 14 with $\Theta = 1$ since the aperture averaging effects are minimal. Table 5 shows σ_s^2 / \bar{s}^2 for $\lambda = 10.6\mu$ m.

Tables 4 and 5 and figures 4b and 4c show that for ranges greater than 5 km or C_N^2 greater than $10^{-15} \text{ m}^{-2/3}$ the scintillation effects can be significant. For example, at 10.6 μ m a direct detection receiver at 5 km with $C_N^2 = 10^{-14} \text{ m}^{-2/3}$ will experience 71% modulation of the received pulse energy. The transmitted laser power must then be four times greater than in the absence of turbulence to assure the same minimum SNR at the receiver.

For slant ranges the effective C_N^2 value is reduced. The value of C_N^2 is known to drop about one order of magnitude in the first 10 to 30 meters above ground. On a day when $C_N^2 = 10^{-14}$ at ground level the effective C_N^2 value at typical ranges or target elevations may then be closer to $10^{-15} \text{ m}^{-2/3}$.

TABLE 4
 NORMALIZED VARIANCE OF SIGNAL AFTER APERTURE AVERAGING
 (Direct Detection, $\lambda = 1.06\mu\text{m}$)

Range, km	$D/(\lambda R)^{1/2}$	θ	σ_s^2 / \bar{s}^2		
			$C_N^2 = 10^{-13} \text{m}^{-2/3}$	$C_N^2 = 10^{-14}$	$C_N^2 = 10^{-15}$
10^{-1}	9.7	4×10^{-3}	$(0.01)^2$	$(0.004)^2$	$(0.001)^2$
1	3.1	3×10^{-2}	$(0.58)^2$	$(0.10)^2$	$(0.03)^2$
5	1.4	10^{-1}	$(1.06)^2$	$(1.06)^2$	$(0.29)^2$
10	0.97	3×10^{-1}	$(1.83)^2$	$(1.83)^2$	$(1.48)^2$
10^2	0.31	8×10^{-1}	$(2.99)^2$	$(2.99)^2$	$(2.99)^2$

TABLE 5
 NORMALIZED VARIANCE OF SIGNAL
 (Direct Detection, $\lambda = 10.6\mu\text{m}$, $\theta = 0.$)

Range, km	$C_N^2 = 10^{-13} \text{m}^{-2/3}$	$C_N^2 = 10^{-14}$	$C_N^2 = 10^{-15}$
10^{-1}	$(0.06)^2$	$(0.02)^2$	$(0.006)^2$
1	$(0.49)^2$	$(0.15)^2$	$(0.05)^2$
5	$(3.34)^2$	$(0.71)^2$	$(0.20)^2$
10	$(3.34)^2$	$(1.79)^2$	$(0.39)^2$
10^2	$(3.34)^2$	$(3.34)^2$	$(3.34)^2$

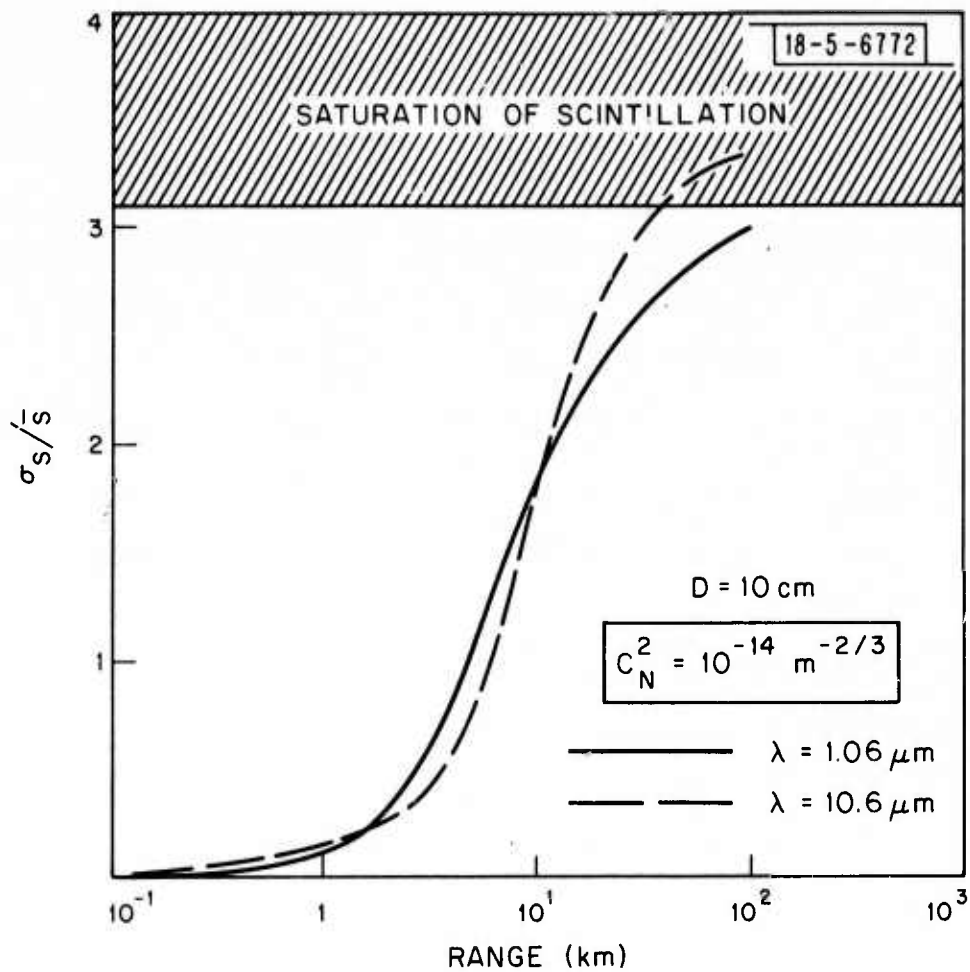


Fig. 4b. Normalized std. deviation of signal due to atmospheric scintillation.

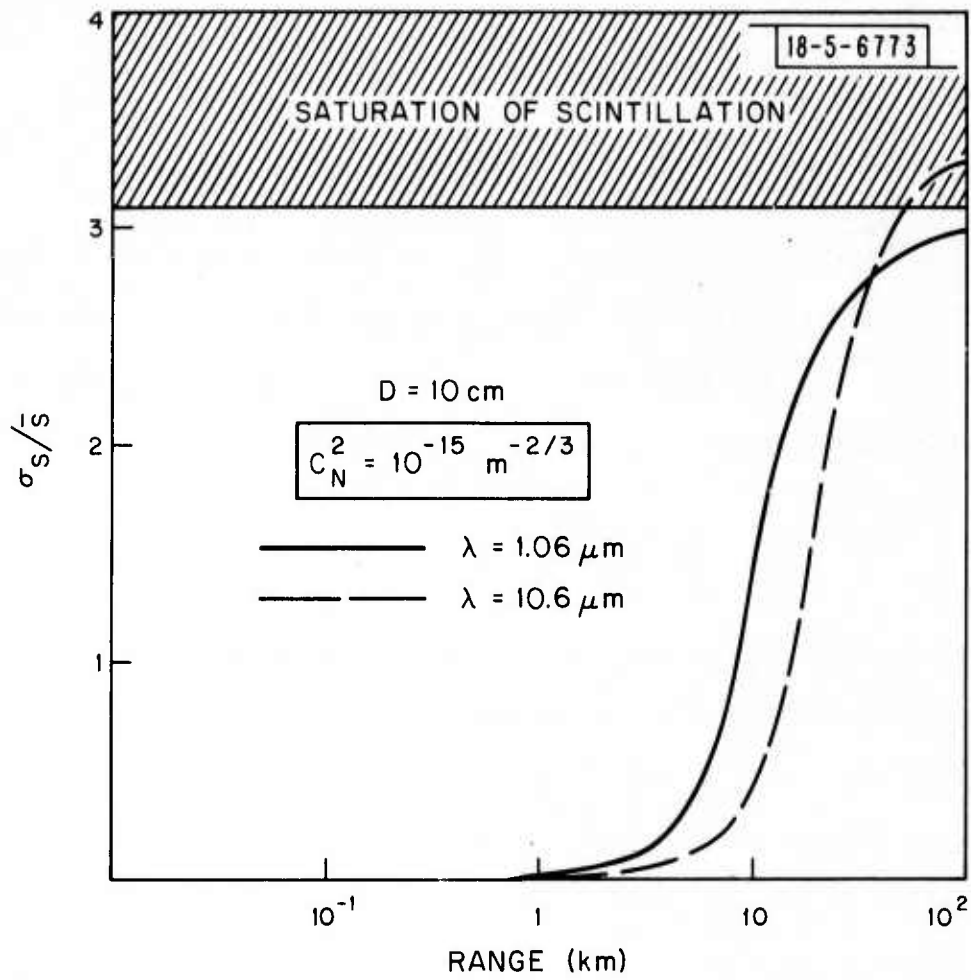


Fig. 4c. Normalized std. deviation of signal due to atmospheric scintillation.

For heterodyne detection the normalized variance of signal power is

$$\frac{\sigma_s^2}{\bar{s}^2} = \left[\phi(D/r_0) \exp(\beta \sigma_{\ln I}^2) \right] - 1 \quad (15)$$

where \bar{s} is the average signal power, $\sigma_{\ln I}^2$ is again the variance of log-intensity given by equation 13, $\phi(D/r_0)$ is a wavefront distortion modulation factor⁶, r_0 is the coherence diameter given by equation 12, D is the receiver aperture diameter, and β is a factor defined as

$$\beta = \begin{cases} 1 & D \ll \sqrt{\lambda R} \\ 0 & D \gg \sqrt{\lambda R} \end{cases} \quad (16)$$

In heterodyne detection, β essentially represents the aperture averaging effects while ϕ represents the wavefront distortion which causes a loss of heterodyne signal conversion efficiency.

Figure 3 shows that at $\lambda = 10.6\mu\text{m}$, D is less than $(\lambda R)^{1/2}$ at all ranges greater than 1 km. Also, reference 6 shows that when $D/r_0 \lesssim 1$ then $\phi \sim 1$. Figure 2 shows that $D \ll r_0$ for all but the most extreme turbulence condition at $\lambda = 10.6\mu\text{m}$. Under these conditions σ_s^2 / \bar{s}^2 becomes the same as equation 14 with $\Theta = 1$. As a result we can conclude that the values of σ_s^2 / \bar{s}^2 in Table 5 represent both heterodyne and direct detection systems at $\lambda = 10.6\mu\text{m}$.

At $\lambda = 1.06\mu\text{m}$ D is greater than $(\lambda R)^{1/2}$ at all ranges up to 10 km so that β is small. There is then some averaging of scintillation. However, equation 12 shows that at this wavelength $D/r_0 \sim 50$ for the 10 cm diameter

receiver aperture. This results in an increase by a factor of 50 in σ_s^2 / \bar{s}^2 . The wavefront distortion introduced by using an aperture much larger than r_0 is therefore another significant argument against the use of heterodyne detection at 1.06 μ m wavelength.

2.4.3 Other Effects

Beam steering, beam spreading, image dancing, and image blurring are also due to turbulence and are closely related to reduction of beam coherence. Beam steering and spreading occur between the transmitter and target, and image dancing and blurring occur between target and receiver.

Beam steering occurs when the angular deviations of instantaneous mean beam position are large in comparison with the angular divergence of the beam. It can cause the beam to miss the target or can reduce the power incident on the target. Beam spreading occurs when the instantaneous wavefront is distorted so that the coherence diameter r_0 is smaller than the beam cross section.

Image dancing occurs when the received instantaneous wavefront is essentially plane over the receiver aperture but the direction of arrival varies randomly over angles greater than λ/D . Image blurring occurs when the coherence diameter r_0 of the return from the target is smaller than the receiver aperture diameter.

All of these effects are related directly to the mean square fluctuation in phase given by

$$\sigma_\phi^2(r) = \left\{ \begin{array}{l} 1.46 \\ 2.92 \end{array} \right\} C_N^2 k^2 R r^{5/3}$$

where 1.46 and 2.92 are for the far field and near field. The corresponding rms fluctuation in angle when the wavefront remains plane is

$$\sigma_{\theta} = \frac{\sigma_{\phi}}{k r}$$

where $k = 2\pi/\lambda$ and r is the separation of two points in the transmitted beam or receiver aperture.

The analysis does not permit separation of the magnitude of beam steering from spreading, or image dancing from blurring. Although the effects are different experimentally, the average effects are equivalent.

The value of σ_{θ} is shown in figure 5 vs. range for the 10 cm diameter transmit/receive aperture. The diffraction limited angles are also indicated for the two wavelengths. Turbulence effects on angular broadening are seen to be negligible at 10.6 μm at ranges up to 10 km for all but the most severe turbulence conditions. At $\lambda = 1.06\mu\text{m}$ the angular broadening is significant for the 10 cm aperture. The effect on a direct detection system is to set a lower limit on the achievable angular resolution or to increase the requirements for angle tracking, or both.

For heterodyne detection systems these effects are shown more directly by the analysis of the section on beam coherence reduction.

3. LASER POWER REQUIREMENTS

The purpose of this section is to determine as a function of range what laser power is required to achieve a minimum SNR_p .

For direct detection the required power is found from equations 5 and

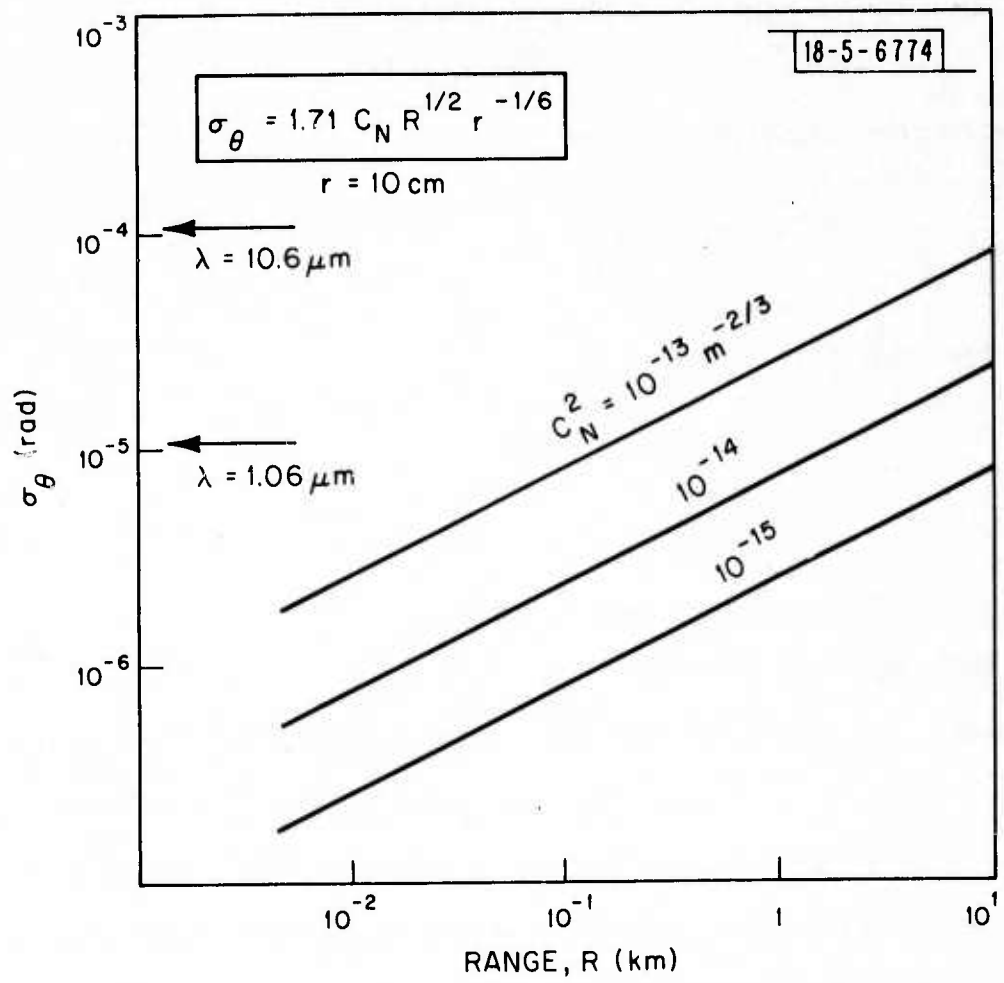


Fig. 5. RMS angular beam spread due to turbulence.

7 to be

$$P_T = (\text{SNR}_p)^{1/2} \cdot \frac{(\text{NEP}/\text{Hz}^{1/2}) \cdot B^{1/2}}{L_R}$$

For heterodyne detection, similarly

$$P_T = \text{SNR}_p \cdot \frac{h \nu B/\eta}{L_R}$$

where the range loss factor L_R is

$$L_R = \frac{\sigma}{\theta^2 R^2} \cdot e^{-2 \alpha R} \cdot \frac{A}{\pi R^2} \cdot \epsilon$$

with the parameters defined by equation 7.

The parameters selected for the required power calculations and determined from the performance analyses of the previous sections are shown in Table 6. The overall approach taken in this analysis is to select parameters which are reasonable based on the results of previous sections. When other parameters are considered, the required laser power can readily be determined from the baseline calculation and the appropriate formula for P_T .

The range loss factor L_R is shown in figure 6. As shown, the loss is somewhat greater for 1.06 μm direct detection with increasing range due to the larger attenuation at this wavelength. At 10 km the loss is approximately 20 dB worse at 1.06 μm than it is at 10.6 μm . This is a significant difference between systems at these two wavelengths.

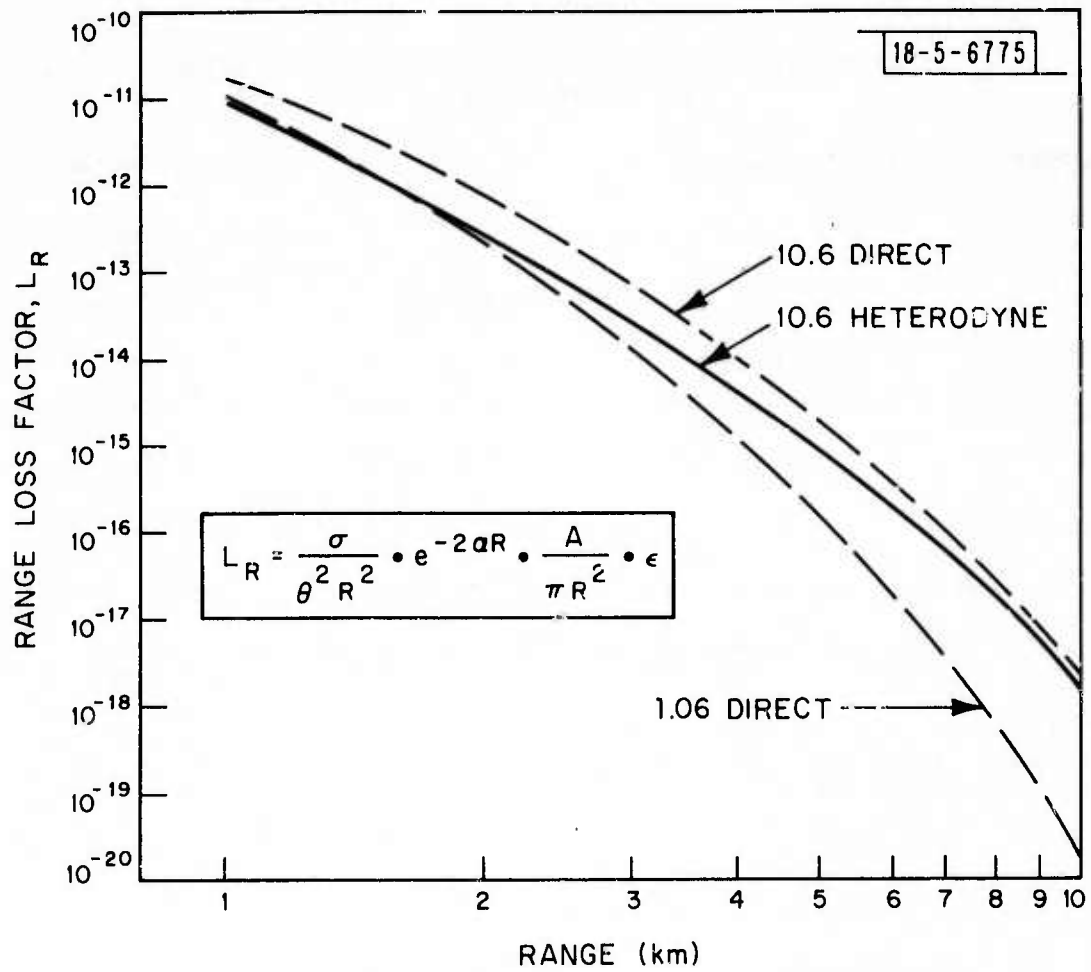


Fig. 6. Range loss factor vs. range.

TABLE 6
SYSTEM PARAMETERS FOR DIRECT AND HETERODYNE SYSTEMS
AT 1.06 and 10.6 μ m

<u>Parameter</u>	<u>1.06 Direct</u>	<u>10.6 Direct</u>	<u>10.6 Heterodyne</u>
σ	10 cm ²	10 cm ²	10 cm ²
θ	10 ⁻⁴ rad	10 ⁻⁴ rad	10 ⁻⁴ rad
α	0.610 km ⁻¹ (2.65 dB/km)	0.357 km ⁻¹ (1.55 dB/km)	0.357 km ⁻¹ (1.55 dB/km)
A	$\pi(10 \text{ cm})^2/4$	$\pi(10 \text{ cm})^2/4$	$\pi(10 \text{ cm})^2/4$
ϵ	0.15	0.15	0.08

To determine P_T it is now necessary to determine NEP/Hz^{1/2} and $h\nu/\eta$. As stated in section 2.1, the NEP/Hz^{1/2} for direct detection has contributions from

- (1) signal shot noise
- (2) background shot noise
- (3) dark current shot noise
- (4) Johnson noise
- (5) amplifier noise

The SNR_p equation for direct detection assumes that signal shot noise is negligible if NEP is to be independent of signal level.

The following calculations assume a silicon avalanche photodiode for 1.06 direct and a HgCdTe photodiode at 10.6 for both heterodyne and direct detection. Photovoltaic operation for 10.6 direct is required to provide

adequate bandwidth for the ranging pulses. For 10.6 μm , $h\nu/\eta = 3.74 \times 10^{-20}$ joule for $\eta = 0.5$.

Table 7 shows the NEP/Hz^{1/2} calculations for the following parameters. At 1.06 μm $G = 125$, $F' - G^{1/2} = 11.2$, $R = \eta q/h\nu = 0.13$, $q = 1.6 \times 10^{-19}\text{C}$, $\eta = 0.15$, $I_D = 10^{-7}\text{a}$, $T = 300\text{K}$, $R = 50\ \Omega$, $F = 2$, $T = 0.15$. At 10.6 μm these parameters are $F' = 1$, $G = 1$, $I_D = 10^{-8}\text{a}$, $R = 4.28$, $\eta = 0.5$, $T = 300\text{K}$, $R = 50\ \Omega$, $F = 2$, $T = .15$. Background power levels are taken from figure 1. Dark current, quantum efficiency, and amplifier noise factors are taken from current representative manufacturers' product literature. The calculations show that for the narrow transmit and receive beam divergences used the direct detection systems are not background limited. The NEP/Hz^{1/2} for the two wavelengths are approximately equal since the higher responsivity at 10.6 μm approximately offsets the lack of a gain mechanism.

TABLE 7
DIRECT DETECTION NEP/Hz^{1/2} at 1.06 and 10.6 μm

Noise	NEP/Hz ^{1/2}	1.06 μm	10.6 μm
background	$(2qF'P_B T/R)^{1/2}$	$1.5 \times 10^{-18}\text{W/Hz}^{1/2}$ (sunlit cloud)	1.0×10^{-19} (300 K)
dark current	$(2qF'I_D/R^2)^{1/2}$	4.6×10^{-12}	1.32×10^{-14}
Johnson	$(4kT/RG^2R^2)^{1/2}$	1.1×10^{-12}	4.2×10^{-12}
amplifier	$[4(F-1)kT_{290}/RG^2R^2]^{1/2}$	1.1×10^{-12}	4.2×10^{-12}
Total	$\left[\sum_i^4 (\text{NEP/Hz}^{1/2})^2 \right]^{1/2}$	4.9×10^{-12}	5.9×10^{-12}

Pulsed Nd:YAG and pulsed CO₂ lasers both produce short pulses of approximately 100 ns in duration. The bandwidth B required for matched filter detection of this pulse is approximately 10⁷ Hz. The range resolution is

$$\Delta R = \frac{C \cdot \tau}{2}$$

where $C = 3 \times 10^8 \text{ m}\cdot\text{s}^{-1}$ and $\tau = 100 \text{ ns}$. The range resolution then is 15 m. This can be improved by leading edge measurement when the SNR_p is much greater than one.¹¹

The SNR_p which yields adequate P_D and FAR is approximately 17 dB or

$$\text{SNR}_p = 50$$

which implies a current or voltage signal to noise ratio of approximately 7.

With the preceding values of B, NEP/Hz^{1/2}, $h \nu/n$, L_R, and SNR_p the required laser transmitter power P_T can be determined. Figure 7 shows P_T for 1.06 direct, 10.6 heterodyne systems, and 10.6 direct.

It is evident from these results that at 5 km the 10.6 heterodyne system has a 4 to 5 order of magnitude power advantage over the 1.06 μm direct system. At 10 km range this advantage becomes from 5 to 6 orders of magnitude. Although there is some power advantage of 10.6 direct detection over 1.06 direct detection the major advantage is realized by employing heterodyne detection at 10.6 μm .

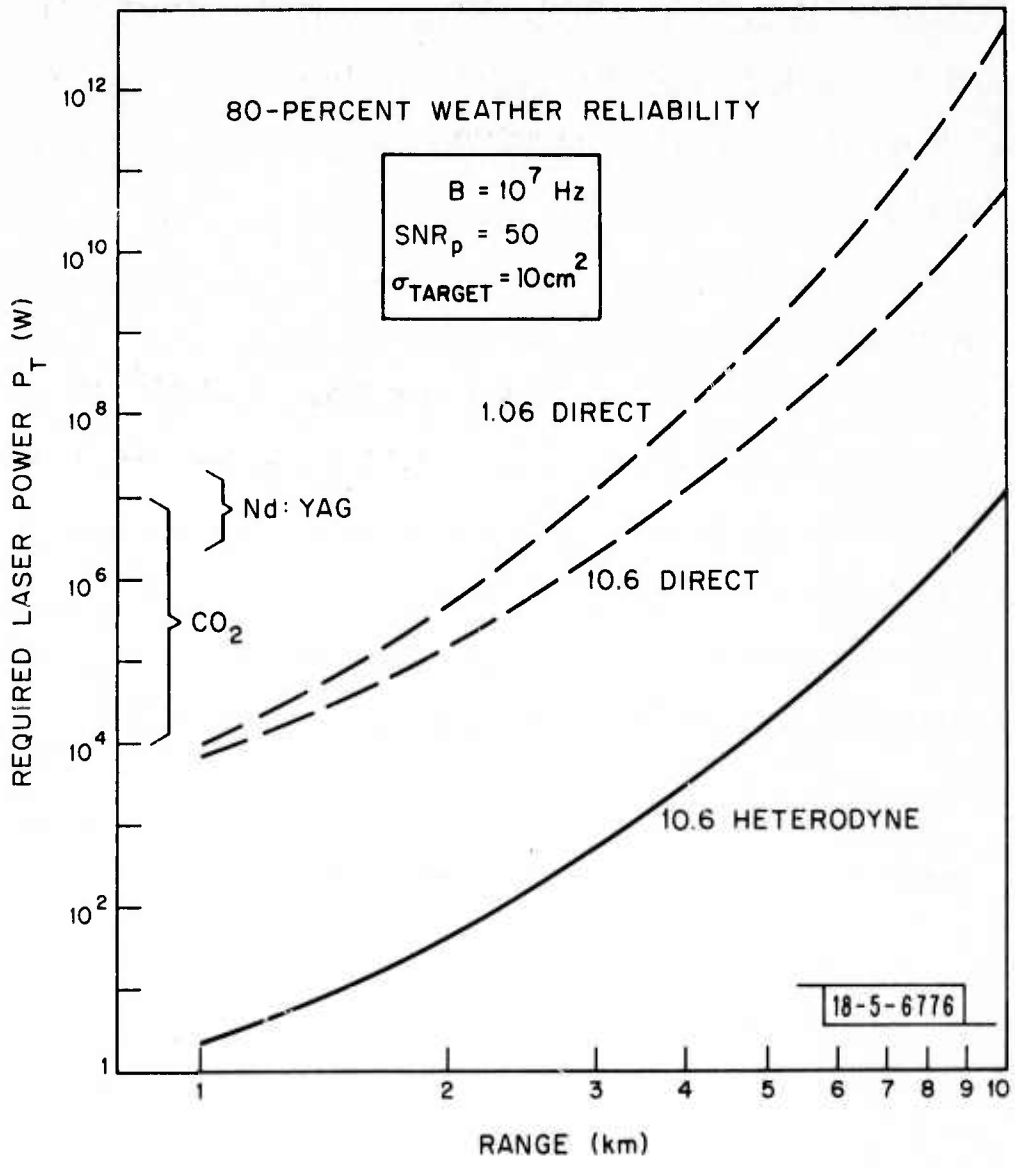


Fig. 7. Required laser power P_T to achieve $SNR_p = 50$.

Presently available Nd:YAG and CO₂ laser power levels are indicated in Figure 7. Figure 7 shows that with the CO₂ laser a heterodyne detection system can reliably achieve operating ranges from 5 to 10 km. On the other hand, a direct detection system using the Nd:YAG laser will not reliably achieve operating ranges greater than 4 km. The range of laser power levels shown for the CO₂ laser represents a range of complexity. Power levels of 10⁷ watts would probably be achieved only with a TEA laser which would involve special power supply requirements.

Some further related considerations regarding laser power levels are the average level power and the laser efficiency. CO₂ lasers typically operate at power conversion efficiencies between 10 and 25%. In comparison, Nd:YAG lasers typically achieve efficiencies of only 1 to 2%.

APPENDIX A

Power Fluctuations Due to Target Surface Roughness

The small amount of measurement data available indicates that many targets of interest have optically smooth surfaces at $10.6\mu\text{m}$. For these targets the conclusions stated in the Introduction apply directly.

When a target is optically rough at the wavelength of interest and when the laser line width is narrow, there is an additional power fluctuation introduced into the received signal. This effect is well known at microwave wavelengths.¹¹ The effect is essentially a random fading of the signal from pulse to pulse.

As a result it is necessary to increase the transmitted pulse power so that even when the return pulse power fades, it will remain high enough to insure a reliable range measurement. The amount of transmitter power increase required depends on the per cent confidence required.

In the case of a heterodyne detection system the envelope fluctuations of the electrical signal current at the intermediate frequency follow a Rayleigh distribution.

The table below shows the required transmitter power increase versus the probability of having enough return power to make the required range measurement using a single pulse.

<u>Probability</u>	<u>Transmit Power Increase</u>
0.50	0
0.90	8.9 db
0.99	19.2 db

Further experimental data regarding the surface roughness characteristics of targets are required to determine whether this added transmitter power is required. With direct detection techniques a power increase would also be required at $10.6\mu\text{m}$ but not at $1.06\mu\text{m}$. However, since the statistics of the signal fluctuations for direct detection are different from the heterodyne detection case, the above values do not apply to direct detection.

REFERENCES

1. W. Wolfe, Ed., Handbook of Military Infrared Technology (Office of Naval Research, Washington, D.C., 1965).
2. T. S. Chu and D. C. Hogg, "Effects of Precipitation on Propagation at 0.63, 3.4, and 10.6 microns," Bell System Tech. J. 47, 5 (1968).
3. R. A. McClatchey et al, "Optical Properties of the Atmosphere," 3d Edition, AFCRL (August 1972).
4. A. Modica and H. Kleiman, "Statistics of Atmospheric IR Transmission," Project Report TT-7, Lincoln Laboratory, M.I.T (3 March 1976).
5. D. L. Fried, "Aperture Averaging of Scintillation," J. Opt. Soc. Am. 57, 169 (1967).
6. D. L. Fried, "Atmospheric Modulation Noise in Heterodyne Receivers," IEEE J. Quantum Electron. QE-3, 213 (1967).
7. R. S. Lawrence and J. W. Strohbehn, "A Survey of Clear Air Propagation Effects Relevant to Optical Communications," Proc. IEEE 58, 1523 (1970).
8. D. L. Fried, "Optical Heterodyne Detection of an Atmospherically Distorted Signal Wave Front," Proc. IEEE 55, 57 (1967).
9. T. J. Gilmartin, R. J. Hull, and L. C. Marquet, "Laser Beam Wander in Atmospheric Propagation," Project Report LTP-7, Lincoln Laboratory, M.I.T. (13 September 1971), DDC AD-896140-L.
10. R. S. Lawrence and J. W. Strohbehn, "A Survey of Clear-Air Propagation Effects Relevant to Optical Communications," Proc. IEEE 58, 1523 (1970).
11. M. I. Skolnik, Introduction to Radar Systems (McGraw-Hill, New York, 1962).

REPORT DOCUMENTATION PAGE		READ INSTRUCTIONS BEFORE COMPLETING FORM	
1. REPORT NUMBER 18 ESD-TR-76-69	2. GOVT ACCESSION NO.	3. RECIPIENT'S CATALOG NUMBER	
6. TITLE (and Subtitle) Pulsed Laser Ranging Techniques at 1.06 and 10.6 um ^{micrometers}		5. TYPE OF REPORT & PERIOD COVERED 9 Project Report	
7. AUTHOR(s) 10 Richard J. Becherer		6. PERFORMING ORG. REPORT NUMBER Project Report TT-8	
9. PERFORMING ORGANIZATION NAME AND ADDRESS Lincoln Laboratory, M.I.T. P.O. Box 73 Lexington, MA 02173		8. CONTRACT OR GRANT NUMBER(s) 15 F19628-76-C-0002	
11. CONTROLLING OFFICE NAME AND ADDRESS Defense Advanced Research Projects Agency 1400 Wilson Boulevard Arlington, VA 22209		10. PROGRAM ELEMENT, PROJECT, TASK AREA & WORK UNIT NUMBERS <input checked="" type="checkbox"/> ARPA Order 2752 Project Element No. 62702E Project No. 6610	
14. MONITORING AGENCY NAME & ADDRESS (if different from Controlling Office) Electronic Systems Division Hanscom AFB Bedford, MA 01731		12. REPORT DATE 11 19 March 1976	
16. DISTRIBUTION STATEMENT (of this Report) Approved for public release; distribution unlimited.		13. NUMBER OF PAGES 48	
14 TT-8		15. SECURITY CLASS. (of this report) Unclassified	
17. DISTRIBUTION STATEMENT (of the abstract entered in Block 20, if different from Report)		15a. DECLASSIFICATION DOWNGRADING SCHEDULE	
18. SUPPLEMENTARY NOTES None		16. HE-6610	
19. KEY WORDS (Continue on reverse side if necessary and identify by block number) target scintillation laser radar range finders		HOWLS Program heterodyne receiver	
20. ABSTRACT (Continue on reverse side if necessary and identify by block number) Heterodyne and direct detection pulsed laser range finders at both 1.06 and 10.6 ^{micrometers} are compared. The application involves a transmitter/receiver at ground level ranging on unresolved high velocity projectiles which appear a few degrees above the horizon at ranges up to 10 km. The analysis includes effects of background, atmospheric turbulence, atmospheric attenuation and target surface characteristics. Available and projected CO ₂ and Nd:YAG laser power levels are assessed to determine expected operating ranges for each system.		MICROMETERS	

207650 ✓

AB